Title
PION PRODUCTION IN NUCLEUS-NUCLEUS COLLISIONS

Author
Pugh, H.G.

Publication Date
1985-10-01

Lawrence Berkeley Laboratory
UNIVERSITY OF CALIFORNIA

Presented at the Symposium on Experimental
Nuclear Physics at Intermediate Energies
Cape Town, South Africa, October 17-18, 1985;
and submitted to the South African Journal of Physics

PION PRODUCTION IN NUCLEUS-NUCLEUS COLLISIONS

H.G. Pugh

October 1985

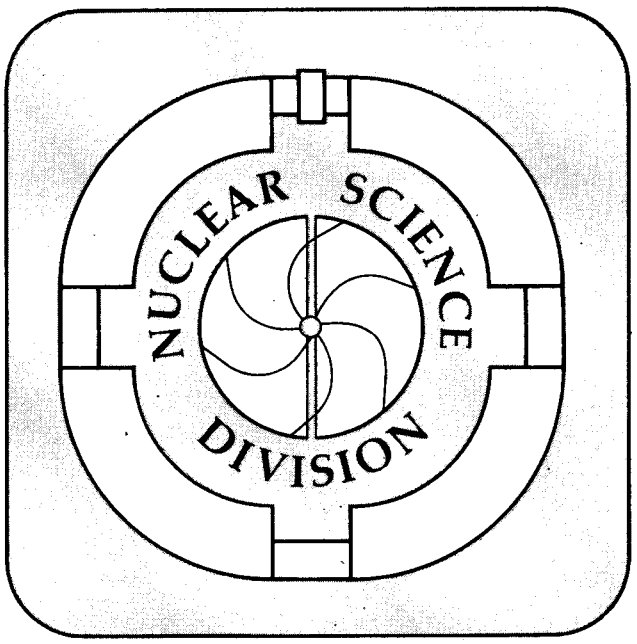

Prepared for the U.S. Department of Energy under Contract DE-AC03-76SF00098

DISCLAIMER

LBL-20373

Pion Production in Nucleus-Nucleus Collisions

Howel G. Pugh

Nuclear Science Division
Lawrence Berkeley Laboratory
University of California
Berkeley, California 94720

Presented at the Symposium on Experimental Nuclear Physics
at Intermediate Energies
Cape Town, South Africa, 17-18 October 1985

Submitted for publication in the South African Journal of Physics

This work was supported by the Director, Office of Energy Research, Division of Nuclear Physics of the Office of High Energy and Nuclear Physics of the U.S. Department of Energy under Contract DE-AC03-76SF00098.

LBL-20373

Pion Production in Nucleus-Nucleus Collisions

Howel G. Pugh

Nuclear Science Division
Lawrence Berkeley Laboratory
University of California
Berkeley, California 94720

Abstract: The experimental investigation of pion production in nucleus-nucleus collisions at the Bevalac is described, with special emphasis on the determination of the nuclear equation of state.

This work was supported by the Director, Office of Energy Research, Division of Nuclear Physics of the Office of High Energy and Nuclear Physics of the U.S. Department of Energy under Contract DE-AC03-76SF00098.

1. Introduction

During the past decade, the observation of pion production has been used extensively as a tool to study the interaction between nuclei at high energies. A strong motivation for these studies was provided by theoretical predictions that the pion yield might depend on the equation of state of nuclear matter and that a sudden change in the yield as a function of energy might signal the occurrence of a phase transition in the hot nuclear matter produced by the collisions.[1] Initial measurements made with nuclear emulsions at the Princeton-Pennsylvania accelerator seemed to show an enormous yield of pions at beam energies below 280 MeV/nucleon.[2] Unfortunately these turned out to be incorrect,[3] and no phase transition has so far been observed, but many interesting results have nevertheless since been found. In particular, pion production has been used to provide a measure of the nuclear equation of state, the first evidence on this at densities above that of the nuclear ground state.

This report will cover the development of an experimental understanding of the main phenomena of pion production in nucleus-nucleus collisions. Even within this limited scope, important sub-areas will have to be omitted. Sub-threshold pion production (i.e., at bombarding energies per nucleon lower than the energy required for production in proton-proton collisions) has recently been studied extensively, with production observed at energies as low as 20 MeV/nucleon.[4] Pion production has been observed at 0° and 180° with pion energies far beyond the kinematic limits of single nucleon-nucleon collisions.[5] An interesting, very strong, enhancement of the π^- yield is observed when the pion momentum equals the velocity of the projectile nucleus;[6] this is believed to occur as a result of coulomb interaction between the pion and fragments of the projectile. Several excellent review articles exist which provide an overview of high energy nucleus-nucleus collisions, and include discussions of these and other topics.[7]

2. Inclusive Spectra

The early measurements of pion production at the Bevalac were of inclusive spectra, i.e., of $d^2\sigma/d\Omega dE$ as a function of pion angle, pion energy, beam energy and target and projectile mass.[8,9] Figures 1, 2 show pion and

proton spectra from the interaction between Ar and KCl at 800 MeV/nucleon. It should be noted that targets such as NaF and KCl are frequently used, rather than pure elements, because they are compatible with streamer chamber operation. The pion spectra show a rapidly-diminishing yield as a function of both pion energy and angle. The proton spectra have a "shoulder-arm" shape, with the "shoulder" disappearing at large angles, while the "arm" behaves rather similarly only to the pion spectra.

To begin to understand these data, it is necessary to know that in a typical nucleus-nucleus collision at non-zero impact parameter, and sufficiently high bombarding energy, there is a rather clean separation between spectators and participants in the reaction. As seen from a head-on viewpoint, the parts of the two nuclei that do not overlap continue largely unaffected by the collision, while the overlapping parts form a highly excited object which has a transient lifetime as a "fireball" but which quickly expands and cools down by emitting its constituent nucleons and created particles, primarily pions. The kinematic regime of the projectile and target fragments is outside the range of the measurements in Figs. 1, 2, where the observed pions and protons should be characteristic of the fireball. The thermodynamic model[10] predicts that the particle spectra should have Maxwell-Boltzmann shape, i.e., $d^2\sigma/dEd\Omega = pE\ d^3\sigma/dp^3 = pE\ \exp(-E/T)$, where p, E are the c.m. momentum and total energy of the observed particle and T is the temperature. If the spectra are analyzed in this form it is found that the extracted temperatures vary with angle. Furthermore, the shoulder in the proton spectra requires an additional ingredient: it is assumed to arise from quasi-free hard nucleon-nucleon scattering processes which do not correspond to thermalization of the participants. The data of reference 9 also included evidence that the pion spectra, especially at forward angles, have a component due to direct Δ-resonance production in nucleon-nucleon collisions, followed by decay of the Δ with pion emission predominantly forwards and backwards in the c.m. systems.

To reduce these effects, Nagamiya et al. chose to analyze spectra only at 90° c.m. for information on temperatures. Figure 3 shows fits to the energy spectra in the Ne + NaF reaction at three beam energies. The slope clearly changes as a function of energy. Figure 4 shows the inverse slope parameter

E_0 as a function of beam energy. Note that it is different for pions and protons, apparently again violating the idea of thermal equilibrium in the fireball. The analysis of reference 9 is slightly flawed by the fact that they fitted $Ed^3\sigma/dp^3$ rather than $d^3\sigma/dp^3$ to an exponential law, but this does not change the results qualitatively.

Many attempts to understand these results met with only partial success. Since each collision has a different impact parameter, the number of participant nucleons and effects due to spectator nucleons, such as pion absorption or rescattering, vary from event to event. With further complications such as production in single nucleon-nucleon collisions, such problems required some additional experimental evidence for their solution. This came in the form of impact-parameter-selected data.

3. Central Collisions

The first studies of central collisions(impact parameter $b \sim 0$) were made using a streamer chamber, which provides a pictorial record of the tracks of all charged particles emitted in each event. Figure 5 shows the layout of the Berkeley streamer chamber. By varying the discriminator threshold on the veto detector T, one can vary the chamber trigger from minimum bias (high discrimination level) to central trigger (low discriminator level). An event in which no fragments of the projectile reach the T detector signals complete destruction of the projectile by the target. For equal-mass target and projectile this means the impact parameter $b = 0$, and all the nucleons in the target and in the projectile form a fireball.

Of course this picture is oversimplified. The nuclear edges are not sharp, and there is, especially for light nuclei, significant transparency in the surface, leading to a "corona" effect in which surface nucleons may undergo few, or no, interactions as the nuclei collide. Apart from this, the triggering procedure is practically ideal, avoiding the use of properties of the fireball itself to define conditions for study of the fireball. In the actual experiment,[11] on interactions between Ar and KCl, the count rate was set to correspond to an interaction cross section of 180 mb, corresponding to $b < 2.4$ fm in a geometrical model which assumes a sharp nuclear surface.

Figure 6 shows the results of studying a large number of streamer chamber photographs, taken in the "inelastic" trigger mode (all impact parameters), or in the "central" trigger mode ($b < 2.4$ fm). For each event the number of negative pions and the total number of charged tracks were measured. For completely central collisions involving total disintegration of both nuclei into individual nucleons we expect about 36 protons plus positive and negative pions. The observed mean value of n_{tot} is 41.8 and the mean value of n_{π^-} is 5.8 for the central collisions. Since the yields of π^+ and π^- are expected to be about the same, total disintegration might give $47.6 = 36 + 5.8 + 5.8$ charged tracks. A closer study of the data reveals that very few events show total disintegration: there must be clusters of nucleons emitted as well as single nucleons. Figure 7 shows the yield of π^- in central collisions of Ar + KCl as a function of beam energy. It shows a smooth dependence on energy, with no steps such as had been predicted for possible phase changes of nuclear matter during the collision process.

Many experiments have been carried out to test if the concept of a fireball is appropriate to the interacting regions of the nuclei. One requirement is that the pion multiplicity should be Poisson distributed about its mean. This is illustrated in Figure 8, again using streamer chamber data from reference 11. However, this is not the only hypothesis that yields a Poisson distribution.[12] Another test using pions is the use of intensity interferometry to study the properties of the emitting source. Careful studies have been made by Zajc et al.[13] In these measurements, events were selected which yielded two pions into the same detector at 45 ± 8 degrees from the beams direction. Such a requirement is found, from independent evidence, to select highly central collisions. The pion pairs were then studied as a function of $\vec{q} = \vec{p}_2 - \vec{p}_1$ and $q_0 = |E_2 - E_1|$ where $\vec{p}$, E are the momentum and energy of the two pions. The results for $2\pi^-$ and $2\pi^+$ emission from ^{40}Ar + KCl at 1.8 GeV/nucleon are shown in Figures 9, 10. If the pions from different points in the source are completely uncorrelated in phase, the correlation in $\vec{q}$ should reach a maximum of 2.0. Its width indicates the spatial extent of the source. Similarly, the correlation in q_0 should also reach 2.0, while its width indicates the temporal extent of the source. The data fall somewhat short of the maximum value of 2.0, indicating some degree of coherence. However, the authors of reference 13 state that

experimental complications prohibit any quantitative conclusions on this point. The spatial and temporal extents of the source have been shown to be reasonable by means of microscopic calculations of the production process.[14)]

4. Temperatures

The study of central collisions allows us to obtain more reliable information on what temperatures are reached in the collision process. The central collision trigger provides a well-defined collision geometry as close to an idealized "fireball" as possible, and it minimizes complications such as spectator matter effects and quasi-free nucleon-nucleon interactions. A careful study of the ^{40}Ar + KCl reaction at 1.8 GeV/nucleon was made by Brockmann et al.[15)] They found that for central collisions the pion and proton angular distributions are much more isotropic than for unbiased events. A remaining forward-backward peaking in the yield could be explained by quasi-free nucleon-nucleon collisions occurring in the nuclear surfaces: the "corona" effect, which cannot be eliminated but could be reduced by studying heavier nuclei, for which the surface is less important. Analyzing the 90° spectra once again minimized this effect and yielded temperature fits shown in Figs 11, 12a for protons and pions respectively. The "temperatures" are found to be extremely different: 118 MeV for the protons and 69 MeV for the pions. If the pion spectrum is analyzed with a two-temperature fit to take account of the excess yield above 0.5 GeV, the "temperature" of the main component drops even lower, to 58 MeV, with a 5% yield at 110 MeV, closer to the proton "temperature." It is interesting to note that the thermodynamical model of Hagedorn and Rafelski[16)] predicts a proton temperature T_p = 120 MeV and a pion temperature T_π = 110 MeV. The slight difference in the temperatures is attributed to the idea that as the fireball expands (and cools) the pions remain in equilibrium somewhat longer than the protons, because of the larger cross sections involved in their scattering. However, the bulk of the observed pions are at T_π = 60-70 MeV, and a new ingredient is required for the explanation.

By contrast, calculations using the intranuclear cascade model (INC) of Cugnon it al.[17)] give an excellent account of the data. Figure 12b shows their predicted spectrum, with a thermal fit to it using T_π = 73 MeV,

close to the 69 MeV which best fit the data. The model predicts T_p = 123 MeV, again close to the observed value. The INC is based on the assumption that the production of pions precedes entirely through the intermediate process Δ production, i.e., $NN \rightarrow N\Delta$; $\Delta \rightarrow N\pi$. The model follows all two-body interactions throughout the collision and within its assumptions is a complete microscopic model of the process. To understand how the large difference between T_π and T_p arises it is instructive to study the kinematics of $\Delta \rightarrow N\pi$, which involves substantial energy release.[18] For a thermal distribution of Δ, with temperature T_Δ, the decay produces a non-thermal distribution of pion and proton energies which can be approximated closely by thermal distributions. The resulting values of T_p and T_π are shown in Figure 13a. To obtain quantitative agreement with the observations it is necessary to realize that the Δ has a large width, and the values of m_Δ produced in the collision depend on the energy available in the nucleon-nucleon system. Calculations within the INC show that the effective m_Δ is, at Bevalac energies, lower than the free value and that it increases with beam energy. Figure 13b shows the dependence of T_p and T_π on m_Δ for fixed T_Δ.

We may conclude that the observations are qualitatively consistent with thermal equilibrium in a fireball consisting primarily of protons and Δ-resonances, both having a temperature of about 120-135 MeV. The "temperatures" extracted from the pion and proton spectra are not the true temperatures, but reflect Δ-decay kinematics. The spectra also have an admixture of particles which do not result from Δ decay but are emitted from thermal equilibration. The INC correctly predicts the final spectra but does not make direct reference to any intermediate equilibrium state. It is instructive, however, to study the progress of the collision as a function of time, as revealed by the INC. Figure 14 shows the most important results (calculations from reference 19) for central collisions ($b \leq 2.4$ fm) of ^{40}Ar + KCl at 977 MeV/nucleon. Figure 14a shows the baryon density in a sphere of 3 fm diameter about the origin of the center-of-mass coordinate system of the participant nucleons, expressed as a ratio to the ground-state nuclear density $\rho_0 = 0.17$ fm^{-3}. It peaks at about 7 fm/c of elapsed reaction time (in the laboratory system), corresponding to the end of the compression stage of the

reaction. Figure 14b shows that about half the baryon-baryon collisions occur during the compression stage and about half during the expansion stage. Figure 14c shows that by the end of the compression stage the total number of pions and delta resonances reaches a plateau where it remains approximately constant throughout the expansion stage. Eventually, after all the Δ resonances have decayed, the number of pions reflects the total number of $\Delta + \pi$ at the maximum compression. Similar calculations on other systems, e.g. La + La,[20] also show this relationship, which will be used in the next section, where the pion yield will be used to extract information on the nuclear system at maximum compression.

5. Effect of Compression on the Pion Yield

So far in this report we have avoided discussion of the absolute yield of pions. Figure 15 shows the mean number of π^- emitted per central collision,[11] previously plotted in Figure 7, but now compared with two theoretical predictions, from an idealized fireball calculation[10] and from the intranuclear cascade calculation.[16,18] Both overpredict the pion yield considerably.

The authors of reference 19 examined the discrepancy between the INC calculation (taken as the most complete microscopic theory of the interaction) and experiment as a function of beam energy and for various combinations of target and projectile. They noticed a strong correlation between the degree of overprediction and the maximum nuclear density reached in the collision, as calculated in the INC. Recalling that the pion yield is determined at the time of maximum compression, they concluded that the discrepancy might be due to the omission of compressional energy from the INC. Thus the pion yield might give direct evidence on the fraction of total energy which is bound up in compressional degrees of freedom and thus not available for pion production. Figure 16 shows how the compressional energy as a function of density is extracted from the data. At each E_{cm} consider the measured multiplicity $\langle n_{\pi^-} \rangle$. In the cascade model this multiplicity is reached at a lower energy, connected by a horizontal arrow in the figure. According to our interpretation, the lower energy corresponds to the kinetic energy remaining available for pion production, while the length of the

horizontal arrow corresponds to E_c, the energy tied up in compressional degrees of freedom, all taken at the time of maximum compression. Unfortunately there is no direct measure of the density, and the INC value has to be assumed correct. Each measurement on Figure 16 then yields a point on Figure 17, where the "measured" compressional energy is plotted against the calculated density. According to the assumptions made, these results represent a measurement of the equation of state of nuclear matter. It is found that the nuclear incompressibility K which fits these data is larger than the value extracted from nuclear monopole vibrations,[21] and corresponds to a "hard" equation of state.

In a subsequent paper,[22] the data were reexamined in a thermodynamic model with Rankine-Hugoniot shock compression in order to see if the results were influenced by the extensive dependence of the above analysis on the results of the INC. Essentially the same results were obtained. Many theoretical papers have examined the assumptions of the analysis, considering the effects of Fermi motion, pion absorption, temperature dependence of the equation of state, etc. A recent survey of the situation is given by Stock.[23] A critical analysis of the problems is given by Sano et al.[24] After applying some corrections to the analysis of reference 18, they compare the results with several theoretical predictions of the nuclear equation of state. These are shown in Figure 18, where it will be noticed how far below the data lie the compressional energies of the "state-of-the-art" conventional nuclear theory prediction represented by the curve FP.[25] The curve B is a typical non-linear mean field theory prediction.[26] The authors of reference 24 examine a wide variety of possible systematic errors in the interpretation and indicate areas requiring further (theoretical) study. This matter is of some importance because of the large discrepancy between the empirical results and conventional nuclear predictions.

6. Supporting Evidence for Compression

In this paper, which concentrates on certain aspects of pion production, the behavior of the nucleonic participants in the collision has been ignored, except for their energy spectra. In fact, when all the outgoing charged

particles are measured simultaneously for each event, a powerful tool for studying compression becomes available. This has been done using the GSI/LBL Plastic Ball,[27] and also by the GSI/LBL Streamer Chamber Collaboration.[28] The outgoing particles are found to exhibit non-spherical patterns of outgoing momentum flow and if these are parameterized in terms of a momentum ellipsoid, a characteristic flow angle is found which depends on impact parameter (determined from participant multiplicity measurements). The results are qualitatively explained in terms of the compressional energy, in a fluid dynamical calculation.[29] There are, however, some difficulties in connecting fluid dynamics results to the experimental data, and the most quantitative conclusions have been obtained using a microscopic theory and studying the same reaction that was used to study pion production. Using a Vlasov-Uehling-Uhlenbeck equation approach[30] the reaction ^{40}Ar + KCl at 1.8 GeV/nucleon as analyzed by a transverse momentum method[31] could be fitted with the same equation of state that fit the pion production data.[32] A useful overview of the entire problem is given in reference 33.

7. Open Questions

The comparison of experimental data with theory for the extraction of information concerning the nuclear equation of state is in its infancy, and the present report has emphasized the theoretical uncertainties to provide a coherent picture of the development of the experimental picture. In so doing several quantities capable of providing useful information have been neglected. For example, the study of particle ratios, e.g. p-d-^{3}H-^{3}He-^{4}He etc., can give evidence on the entropy of the system.[34] This requires much further work from both experimental and theoretical points of view. Another open question is the question of radial flow, suggested originally as a blast-wave theory.[35] This could change the energy balance considerably, and alter our interpretation of the pion and proton energy spectra.[15] In most of the measurements made to date radial flow is confused with other quantities.

Rapid further development of the field is likely, because of significant improvements in experimental capabilities. The Bevalac has recently (1982) been improved to accelerate all nuclei, and experimental data are being

extended to much heavier nuclear systems. In 1986, two new facilities will come into operation for heavy ion physics: the Brookhaven AGS and the CERN SPS. Much of the effort at the latter two will be devoted to searches for a phase transition of nuclear matter to a quark gluon plasma.

In the midst of all this excitement it is a pleasure to welcome the National Accelerator Centre into the ranks of competitors and collaborators in the quest to understand that most important part of our environment, the atomic nucleus.

Acknowledgments

I am grateful to Daan Reitmann and Anthony Cowley for giving me the opportunity to present this paper.

This work was supported by the Director, Office of Energy Research, Division of Nuclear Physics of the Office of High Energy and Nuclear Physics of the U.S. Department of Energy under Contract DE-AC03-76SF00098.

References

1) G. Chapline, M. Johnson, E. Teller, and M. Wiess, Phys. Rev. D8, 4302 (1973);
W. Scheid, H. Müller, and W. Greiner, Phys. Rev. Lett. 32, 741 (1974);
M. Sobel, P.J. Siemens, J.P. Bondorf, and H.A. Bethe, Nucl. Phys. A251, 502 (1975);
Y. Kitazoe, M. Sano and H. Toki, Lett. Nuovo Cimento 13, 139 (1975);

2) P.J. McNulty, G.E. Farrell, R.C. Filz, W. Schimmerling, and K.G. Vosburgh, Phys. Rev. Lett. 38, 1519 (1977).

3) R. Kullberg, A. Oscarsson and I. Otterlund, Phys. Rev. Lett. 40, 289 (1978).

4) T. Johansson, H.. Gustafsson, B. Jakobsson, P. Kristiansson, B. Noren, A. Oskarsson, L. Carlen, J. Julien, C. Guet, R. Bertholet, M. Manuel, H. Nifenecker, P. Perrin, F. Schussler, G. Tibell, M. Buenerd, J.M. Loiseau, P. Martin, J.P. Bondorf, O.-B. Nielsen, A.O.T. Karvinen, and J. Mougey, Phys. Rev. Lett. 48, 732 (1982);
P. Braun-Munzinger, P. Paul, L. Ricken, J. Stachel, P. H. Zhang, G.R. Young, F.E. Obenshain, and E. Grosse, Phys. Rev. Lett. 52, 255 (1984);
H. Noll, E. Grosse, P. Braun-Munzinger, H. Dabrowski, H. Heckwolf, U. Klepper, C. Michel, W.F.J. Muller, H. Stelzer, C. Brendel, and W. Rosch, Phys. Rev. Lett. 52, 1284 (1984).

5) E. Moeller, L. Anderson, W. Brückner, S. Nagamiya, S. Nissen-Meyer, L. Schroeder, G. shapiro, and H. Steiner, Phys. Rev. C28, 1246 (1983); L.S. Schroeder, S.A. Chessin, J.V. Geagon, J.Y. Grossiord, J.W. Harris, D.L. Hendrie, R. Treuhaft, and K. Van Bibber, Phys. Rev. Lett. 43, 1787 (1979); S.A. Chessin, Ph.D. thesis, Lawrence Berkeley Laboratory Report No. LBL-14262 (1983), unpublished.

6) J.P. Sullivan, J.A. Bistirlich, H.R. Bowman, R. Bossingham, T. Buttke, K.M. Crowe, K.A. Frankel, C.J. Martoff, J. Miller, D.L. Murphy, J.O. Rasmussen, W.A. Zajc, O. Hashimoto, M. Koike, J. Peter, W. Benenson, G.M. Crawley, E. Kashy, and J.A. Nolen, Jr., Phys. Rev. C25, 1499 (1982).

7) E.g., S. Nagamiya and M. Gyulassy, Advances in Nuclear Physics vol. 13, ed. J.W. Negele and E. Vogt (Plenum Pub. Corp., New York, (1984) p. 201; also references 23,33. The most recent workshop report is Proceedings of the 7th High Energy Heavy Ion Study, ed.R. Bock, H. Gutbrod, and R. Stock, GSI Report 85-10 (1985).

8) S.Y. Fung, W. Gorn, G.P. Kiernan, F.F. Liu, J.J. Lu, Y.T. Oh, J. Ozawa, R.T. Poe, L. Schroeder, and H. Steiner, Phys. Rev. Lett. 40, 292 (1978).

9) S. Nagamiya, M.-C. Lemaire, E. Moeller, S. Schnetzer, G. Shapiro, H. Steiner, and I. Tanihata, Phys Rev. C24. 971 (1981).

10) R. Hagedorn and J. Ranft, Suppl. Nuovo Cimento 6, 169 (1968); J. Gosset, H.H. Gutbrod, W.G. Meyer, A.M. Poskanzer, A. Sandoval, R. Stock and G.D. Westfall, Phys. Rev. C16, 629 (1977); J. Gosset, J.I. Kapusta and G.D. Westfall, Phys. Rev. C18, 844 (1978).

11) A. Sandoval, R. Stock, H.E. Stelzer, R.E. Renfordt, J.W. Harris, J.P. Brannigan, J.V. Geaga, L.J. Rosenberg, L.S. Schroeder, and K.L. Wolf, Phys. Rev. Lett. 45, 874 (1980).

12) M. Gyulassy and S.K. Kauffmann, Phys. Rev. Lett. 40, 298 (1978).

13) W.A. Zajc, J.A. Bistirlich, R.R. Bossingham, H.R. Bowman, C.W. Clawson, K.M. Crowe, K.A. Frankel, J.G. Ingersoll, J.M. Kurck, C.J. Martoff, D.L. Murphy, J.O. Rasmussen, J.P. Sullivan, E. Yoo, O. Hashimoto, M. Koike, W.J. McDonald, J.P. Miller, and P. Trüol, Phys. Rev. C29, 2173 (1984).

14) T.J. Humanic, LBL-19420 (1985), submitted for publication in Physical Review C.

15) R. Brockmann, J.W. Harris, A. Sandoval, R. Stock, H. Stroebele, G. Odyniec, H.G. Pugh, L.S. Schroeder, R.E. Renfordt, D. Schall, D. Bangert, W. Rauch, and K.L. Wolf, Phys. Rev. Lett. 53, 2012 (1984).

16) R. Hagedorn and J. Rafelski, Phys. Lett. 97B, 136 (1980).

17) J. Cugnon, D. Kinet and J. Vandermeulen, Nucl. Phys. 7379, 553 (1982); J. Cugnon, T. Mitzutani and J. Vandermeulen, Nucl. Phys. A352, 505 (1981).

18) R. Hagedorn, CERN preprint TH 3684 (1984).

19) R. Stock, R. Bock, R. Brockmann, J.W. Harris, A. Sandoval, H. Stroebele, K.L. Wolf, H.G. Pugh, L.S. Schroeder, M. Maier, R.E. Renfordt, A. Dacal, and M.E. Ortiz, Phys. Rev. Lett. 49, 1236 (1982).

20) J.W. Harris and R. Stock, LBL report 17054 (1984).

21) F. Serr, G. Bertsch and J.P. Blaizot, Phys. Rev. C22, 922 (1980).

22) J.W. Harris, R. Bock, R. Brockmann, A. Sandoval, R. Stock, H. Stroebele, G. Odyniec, H.G. Pugh, L.S. Schroeder, R.E. Renfordt, D. Schall, D. Bangert, W. Rauch, and K.L. Wolf, Phys. Lett. 153B, 377 (1985).

23) R. Stock, Lectures at the Erice Nuclear Physics School, Erice, Italy, April 10-22, 1985; GSI preprint 85-39 (1985).

24) M. Sano, M. Gyulassy, M. Wakai, and Y. Kitazoe, Phys. Lett. 156B, 27 (1985).

25) B. Friedman and V.R. Pandharipande, Nucl. Phys. A361, 502 (1981).

26) J. Boguta and H. Stocker, Phys. Lett. 120B, 289 (1983).

27) H.A. Gustafsson, H.H. Gutbrod, B. Kolb, H. Loehner, B. Ludewigt, A.M. Poskanzer, T. Renner, H. Riedesel, H.G. Ritter, A. Warwick, F. Weik and H. Wieman, Phys. Rev. Lett. 52, 1590 (1984).

28) R.E. Renfordt, D. Schall, R. Bock, R. Brockmann, J.W. Harris, A. Sandoval, R. Stock, H. Stroebele, D. Bangert, W. Rauch, G. Odyniec, H.G. Pugh, and L.S. Schroeder, Phys. Rev. Lett. 53, 763 (1984).

29) G. Buchwald, G. Graebner, J. Theis, J. Maruhn, W. Greiner, and H. Stocker, Phys. Rev. Lett. 52, 1594 (1984).

30) H. Kruse, B.V. Jacak, J.J. Molitoris, G.D. Westfall, and H. Stocker, Phys. Rev. C31, 1770 (1985).

31) P. Danielewicz and G. Odyniec, Phys. Lett. 157B, 146 (1985).

32) J.J. Molitoris and H. Stocker, Phys. Rev. C32, 346 (1985).

33) J.J. Molitoris, D. Hahn and H. Stocker, Lectures at the Erice Nuclear Physics School, Erice, Italy, April 10-22, 1985; Michigan State University preprint MSUCL-530 (1985).

34) P.J. Siemens and J.I. Kapusta, Phys. Rev. Lett. 43, 1486 (1979); K.G.R. Doss, H.A. Gustafsson, H.H. Gutbrod, B. Kolb, H. Löhner, B. Ludewigt, A.M. Poskanzer, T. Renner, H. Riedesel, H.G. Ritter, A. Warwick, and H. Wieman, Phys. Rev. C32, 116 (1985).

35) P.J. Siemens and J.O. Rasmussen, Phys. Rev. Lett. 42, 880 (1979).

Figures

Figure 1. Inclusive spectra of π^- in 800 MeV/nucleon ^{40}Ar + KCl collisions (reference 9). Note that the quantity plotted is the Lorentz-invariant cross section.

Figure 2. Inclusive spectra of protons in 800 MeV/nucleon ^{40}Ar + KCl collisions (reference 9).

Figure 3. Proton and π^- energy spectra at $\theta_{cm} = 90°$ in ^{20}Ne + NaF collisions at 0.4, 0.8 and 2.1 GeV/nucleon. E_o is the slope factor when the cross sections are parameterized by $\exp(-E_k^*/E_o)$ when E_k^* is the proton (or pion) kinetic energy in the c.m. frame (reference 9).

Figure 4. Exponential slope factors E_o from Figure 3, plotted as a function of the beam energy per nucleon in the c.m. frame (reference 9).

Figure 5. System used in the minimum bias and central trigger runs with the streamer chamber. C, S_1, S_2, S_3 and T are scintillators. The beam is prepared by the signal $B = S_1 \cdot S_2 \cdot S_3 \cdot \bar{C}$. The trigger is defined as the beam in anti-coincidence with the trigger scintillator above a certain threshold ($B \cdot \bar{T}$).

Figure 6. Total charged particle (n_{tot}) and negative pion (n_{π^-}) multiplicity distributions for the interaction of ^{40}Ar + KCl at 1.8 GeV/nucleon for the inelastic (•) and central (□) trigger modes. Representative error bars are shown and the curves are drawn to guide the eye (reference 11).

Figure 7. Center-of-mass energy dependence of the mean negative pion multiplicity $\langle n_{\pi^-} \rangle$ for central collisions of ^{40}Ar + KCl corresponding to a constant σ_n = 180 mb. The dashed line is shown to guide the eye (reference 11).

Figure 8. Distribution of n_{π^-} for central ^{40}Ar + KCl collisions at 1.8 GeV/nucleon (reference 11). The curve shows a Poisson distribution of mean 5.81.

Figure 9. Intensity interferometry correlation functions for ^{40}Ar + KCl at 1.8 GeV/nucleon yielding $2\pi^-$ near 45°. Data from reference 13, including corrections for the Coulomb repulsion of the pions. The curves represent a fit to the data.

Figure 10. Same as Figure 9 except for $2\pi^+$.

Figure 11. Proton energy spectrum of central ^{40}Ar + KCl collisions at 1.8 GeV/nucleon fitted with a thermal model prediction for T = 118 MeV (reference 15).

Figure 12. (a) π^- energy spectrum of central ^{40}Ar + KCl collisions at 1.8 GeV/nucleon fitted with a thermal model prediction for T_π = 69 MeV, (b) Predictions of the intranuclear cascade model of Cugnon et al. for the π^- energy spectrum. The curve represents a fit to the calculated spectrum using T_π = 73 MeV (reference 15).

Figure 13. (a) Dependence of pion and proton temperatures T_π and T_p on Δ temperature for m_Δ = 1232 MeV, (b) Dependence of T_π and t_p on M_Δ for T_Δ = 135 MeV.

Figure 14. Results of a cascade calculation for near-central collisions ($b \leq$ 2.4 fm) of ^{40}Ar + KCl at a laboratory bombarding energy of 977 MeV/nucleon. The time dependence of the reactions is shown for (a) the baryon density, relative to the ground-state value, (b) the integrated number of baryon-baryon collisions, and (c) the instantaneous number of pions and Δ resonances.

Figure 15. Center-of-mass energy dependence of the mean negative pion multiplicity $\langle n_\pi^- \rangle$ for central collisions of ^{40}Ar + KCl corresponding to a constant σ_R = 180 mb ($b \leq 2.4$ fm), taken from reference 11. The dashed line shows a fireball prediction[10] and the full line the prediction of the INC.[16,18)]

Figure 16. The mean pion multiplicity as a function of bombarding energy for near central collisions of ^{40}Ar + KCl. The triangles show the data. Open circles show the results of intranuclear cascade calculations. Horizontal arrows show the values of E_c, the compressional energy per nucleon determined from each experimental point (reference 18).

Figure 17. Values of E_c as a function of mean baryon density calculated in the intranuclear cascade model. The dashed lines show equations of state with incompressibility constants K of 250 MeV and 200 MeV, respectively (reference 16).

Figure 18. The energy per baryon at zero temperature as a function of density (reference 24). The shaded region is the empirical result of Figure 17, with some theoretical corrections. The curve FP is from a modern variational calculation;[25] the curve B is typical of non-linear mean field models and is taken from reference 26 with K^{∞} = 240 MeV and m^*/m = 0.65. Curves 3 and 4 correspond to equations of state used in shock calculations for c.m. energies between 0.1 and 0.4 GeV/nucleon.

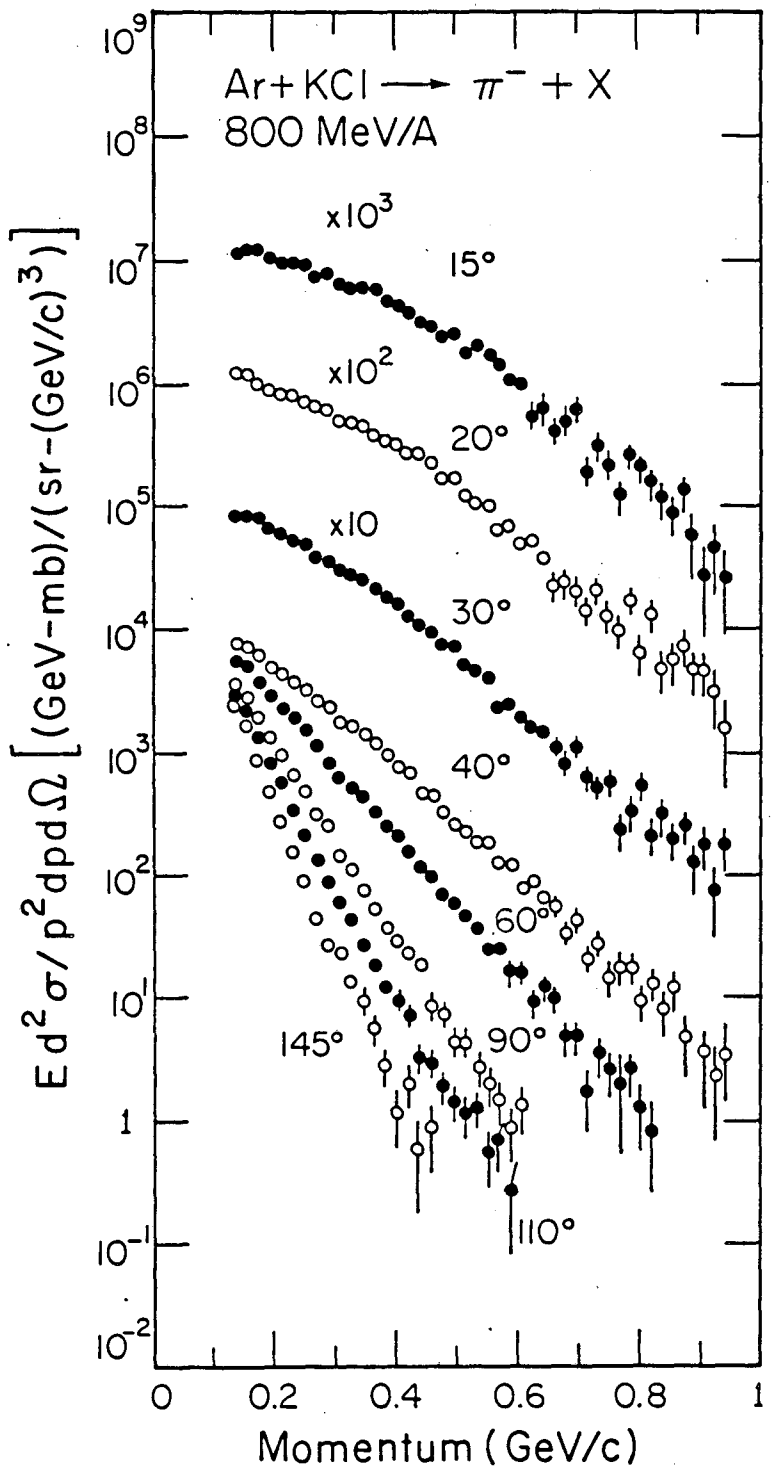

XBL8011-2398

Figure 1

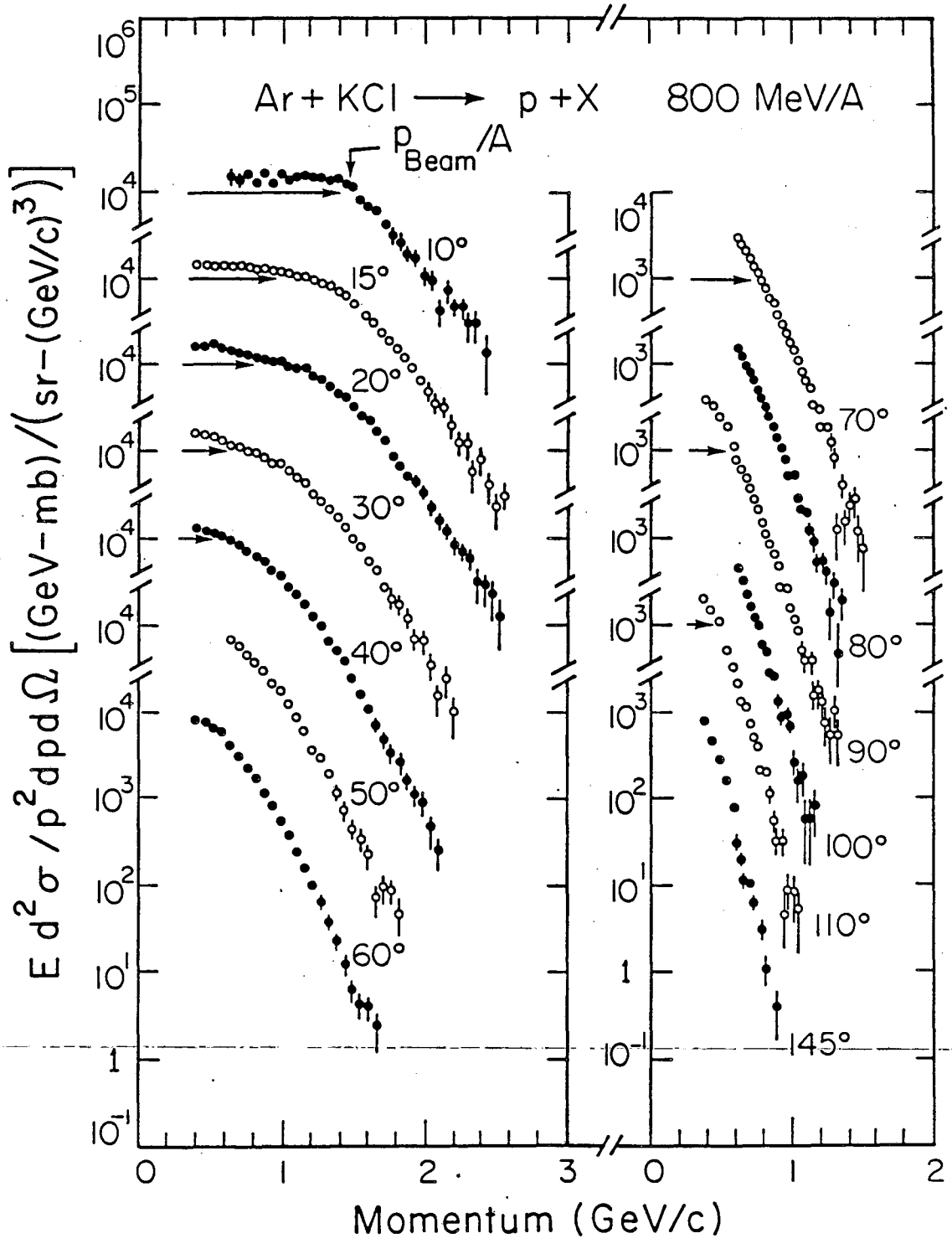

XBL 8011-2393

Figure 2

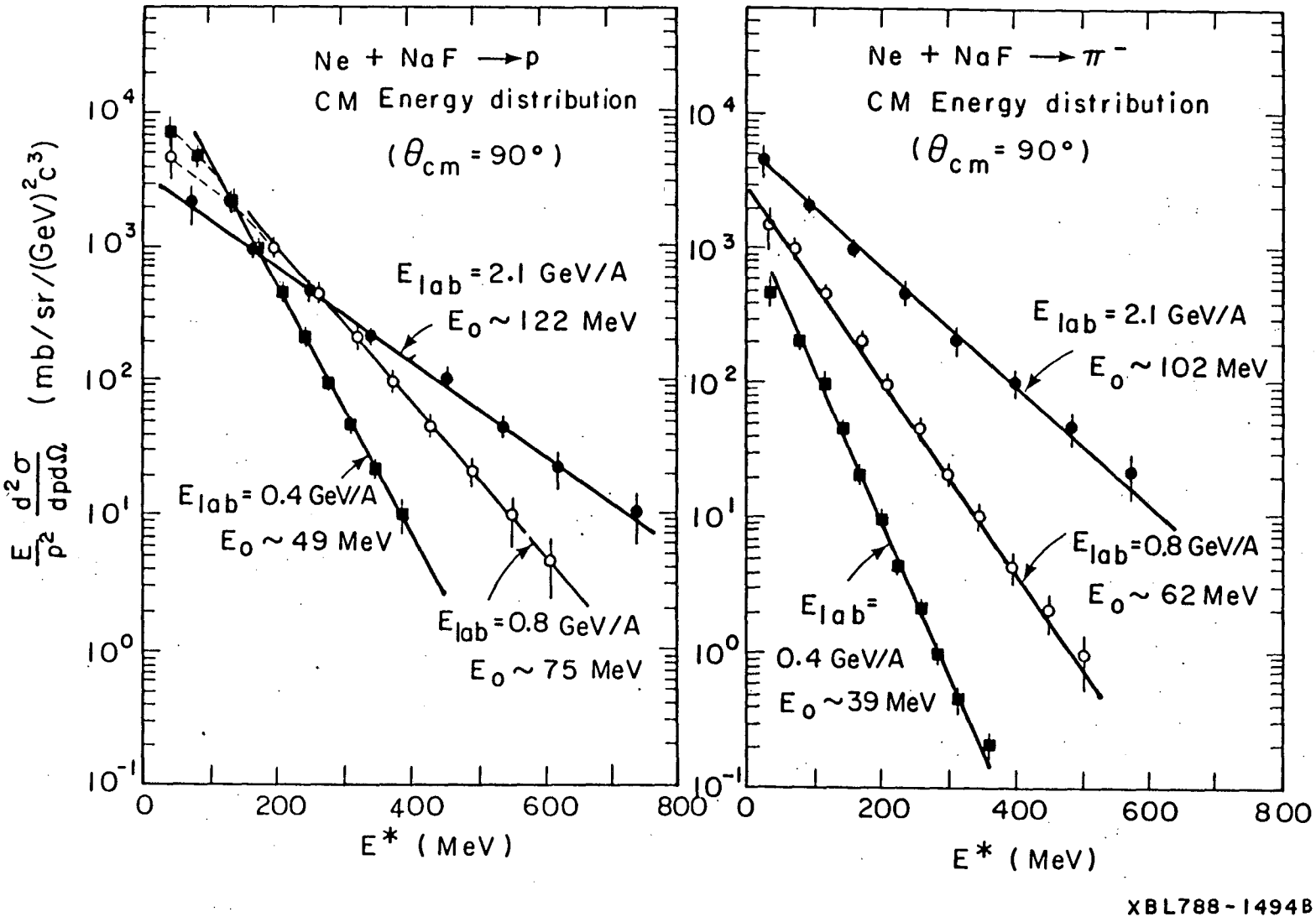
Ne + NaF → p
CM Energy distribution
(θ_{cm} = 90°)
E_{lab} = 2.1 GeV/A
E_o ~ 122 MeV
E_{lab} = 0.4 GeV/A
E_o ~ 49 MeV
E_{lab} = 0.8 GeV/A
E_o ~ 75 MeV
$\frac{E}{p^2}\frac{d^2\sigma}{dpd\Omega}$ (mb/sr/(GeV)^{2}c^3)
E* (MeV)
Ne + NaF → π^-
CM Energy distribution
(θ_{cm} = 90°)
E_{lab} = 2.1 GeV/A
E_o ~ 102 MeV
E_{lab} = 0.8 GeV/A
E_o ~ 62 MeV
E_{lab} = 0.4 GeV/A
E_o ~ 39 MeV
E* (MeV)
XBL788-1494B

Figure 3

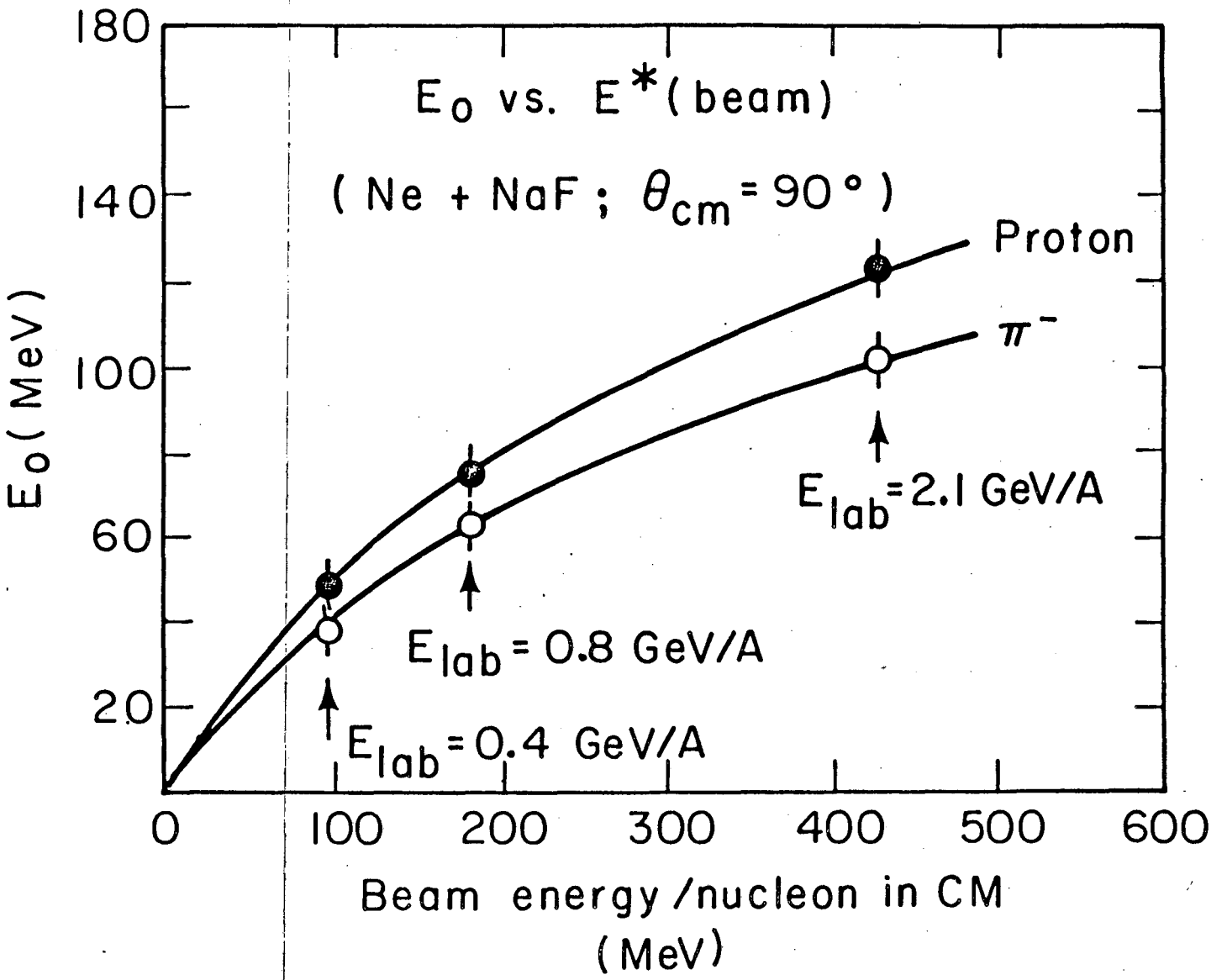

XBL788-1495B

Figure 4

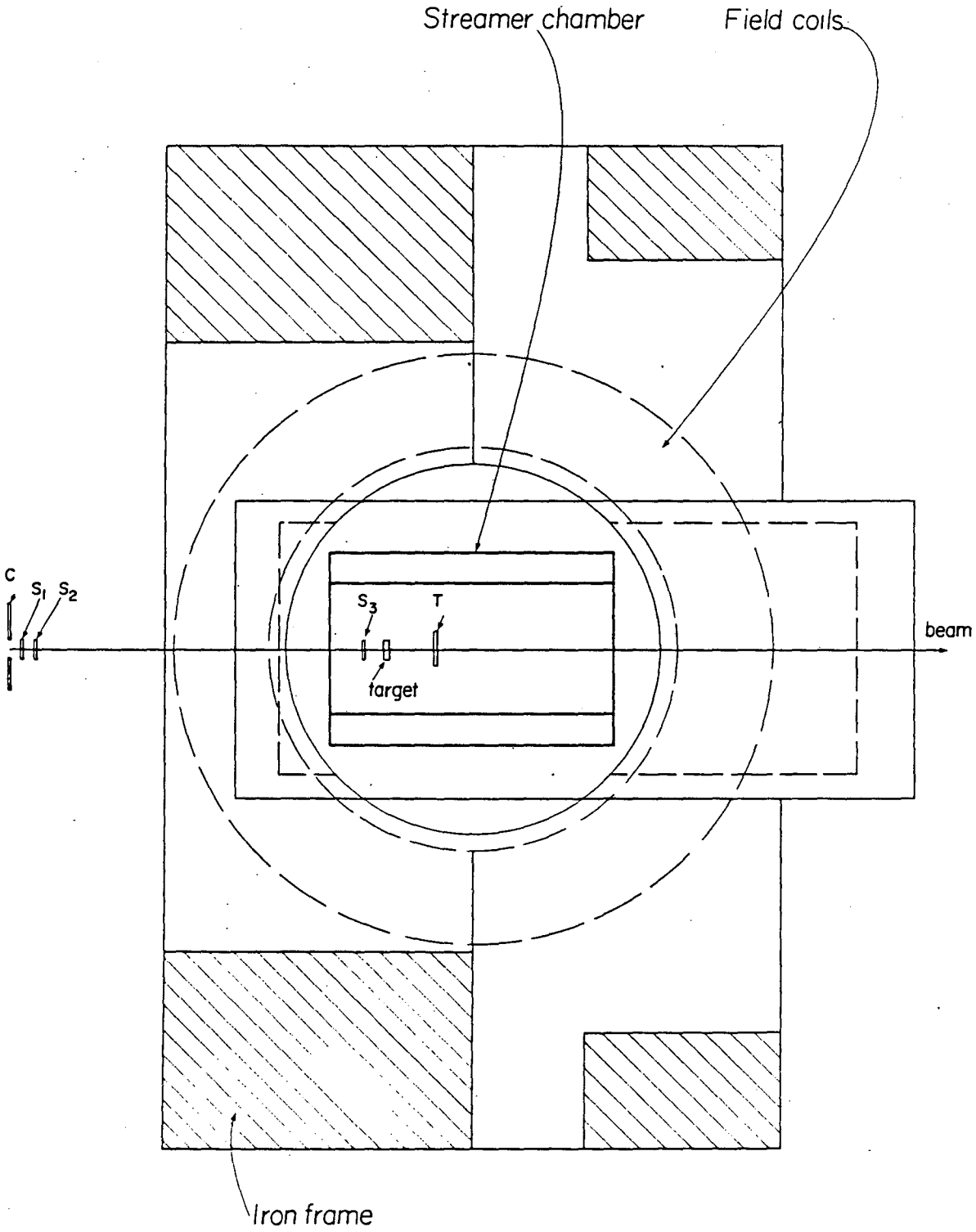
Streamer chamber
Field coils
C
S1
S2
S3
T
target
beam
Iron frame
XBL 817-1054

Figure 5

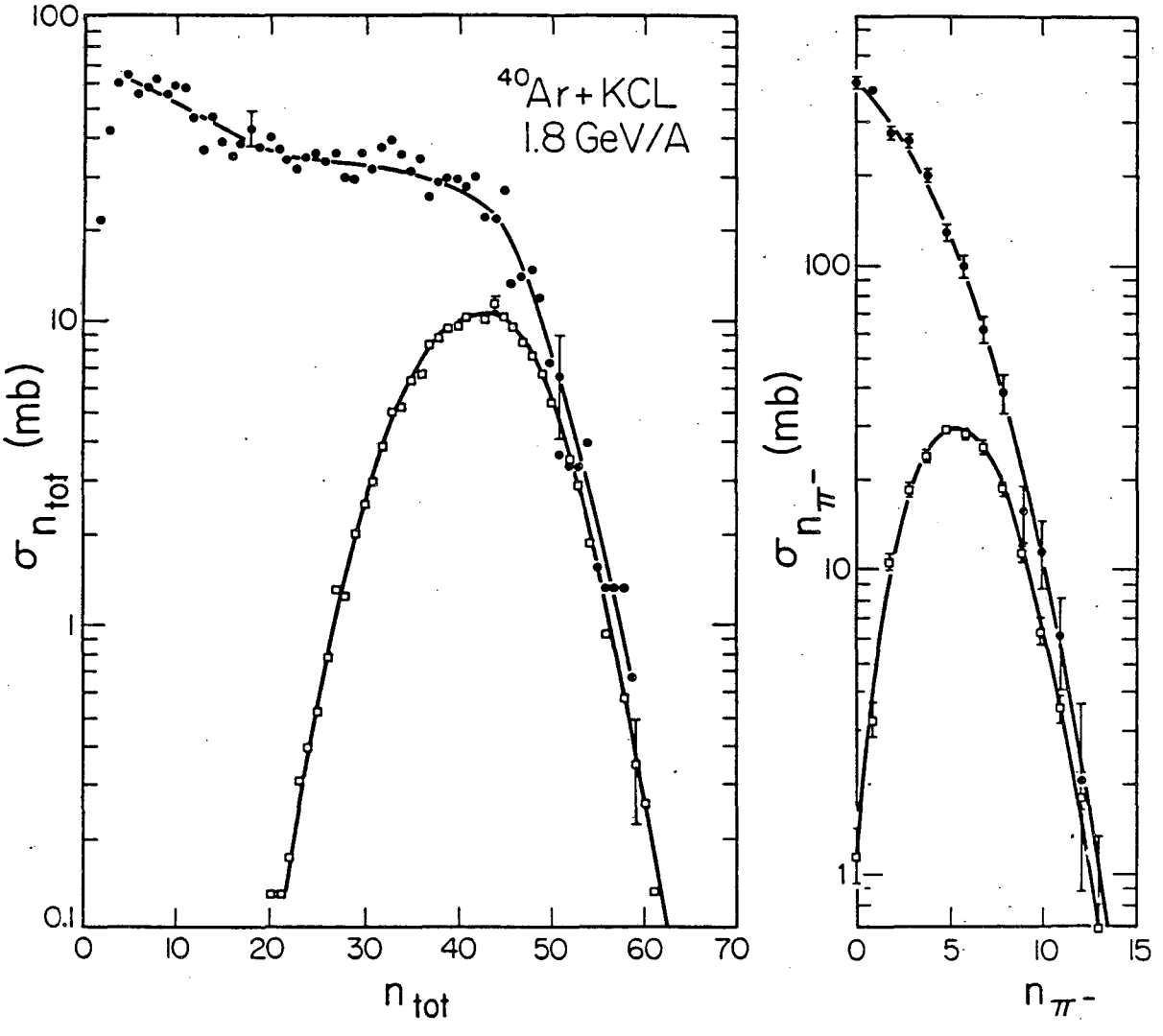

XBL 804-704

Figure 6

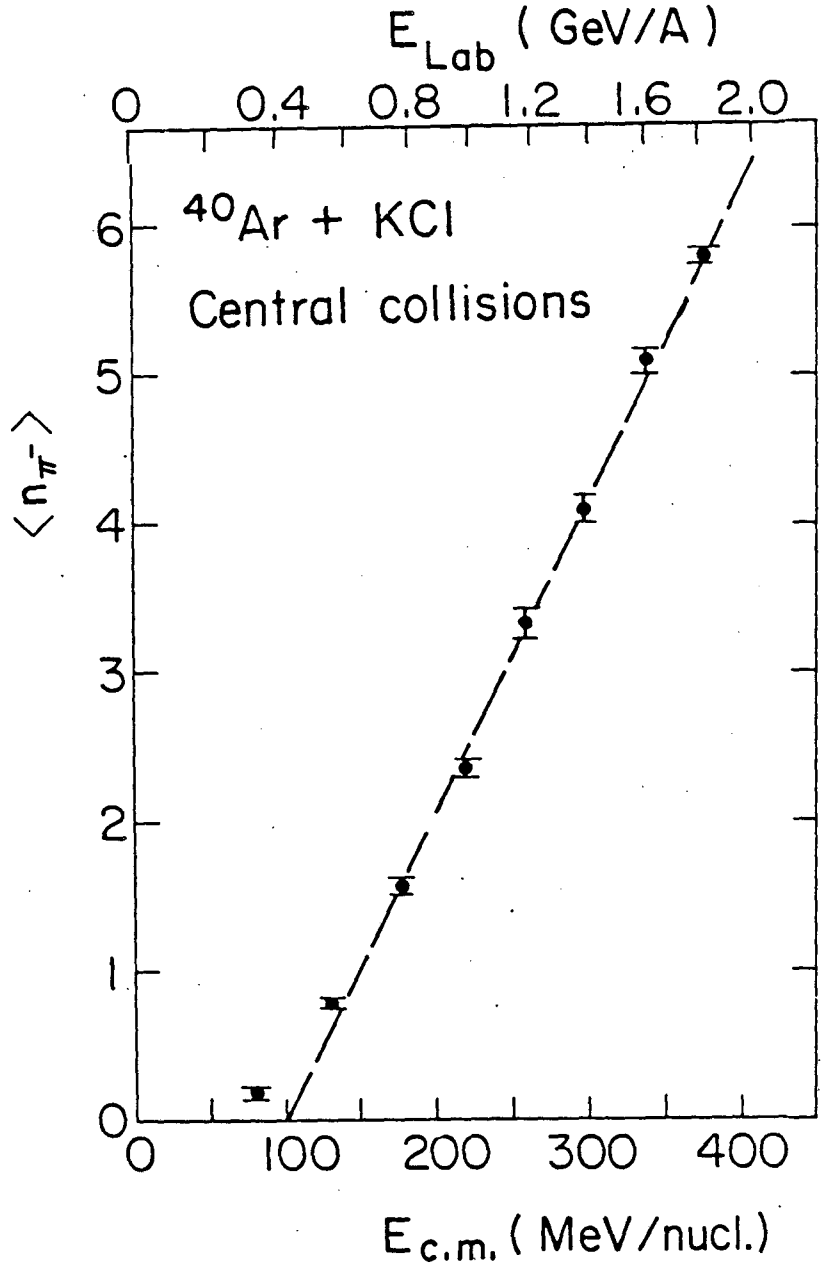

XBL 804-701

Figure 7

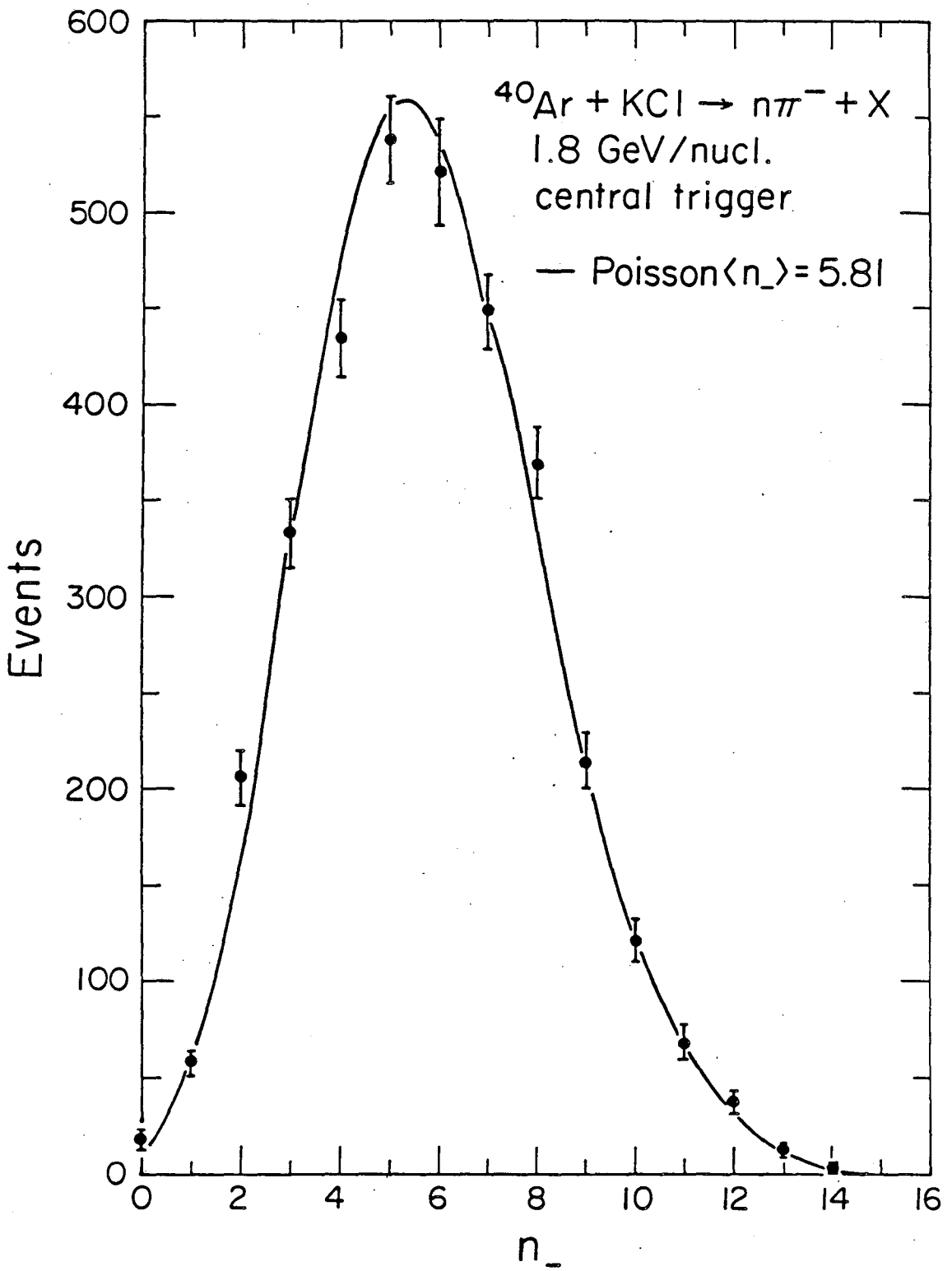
600
500
400
300
200
100
0
Events
0
2
4
6
8
10
12
14
16
n_
$^{40}Ar + KCl \rightarrow n\pi^- + X$
1.8 GeV/nucl.
central trigger
— Poisson⟨n_⟩= 5.81
XBL 822-4454

Figure 8

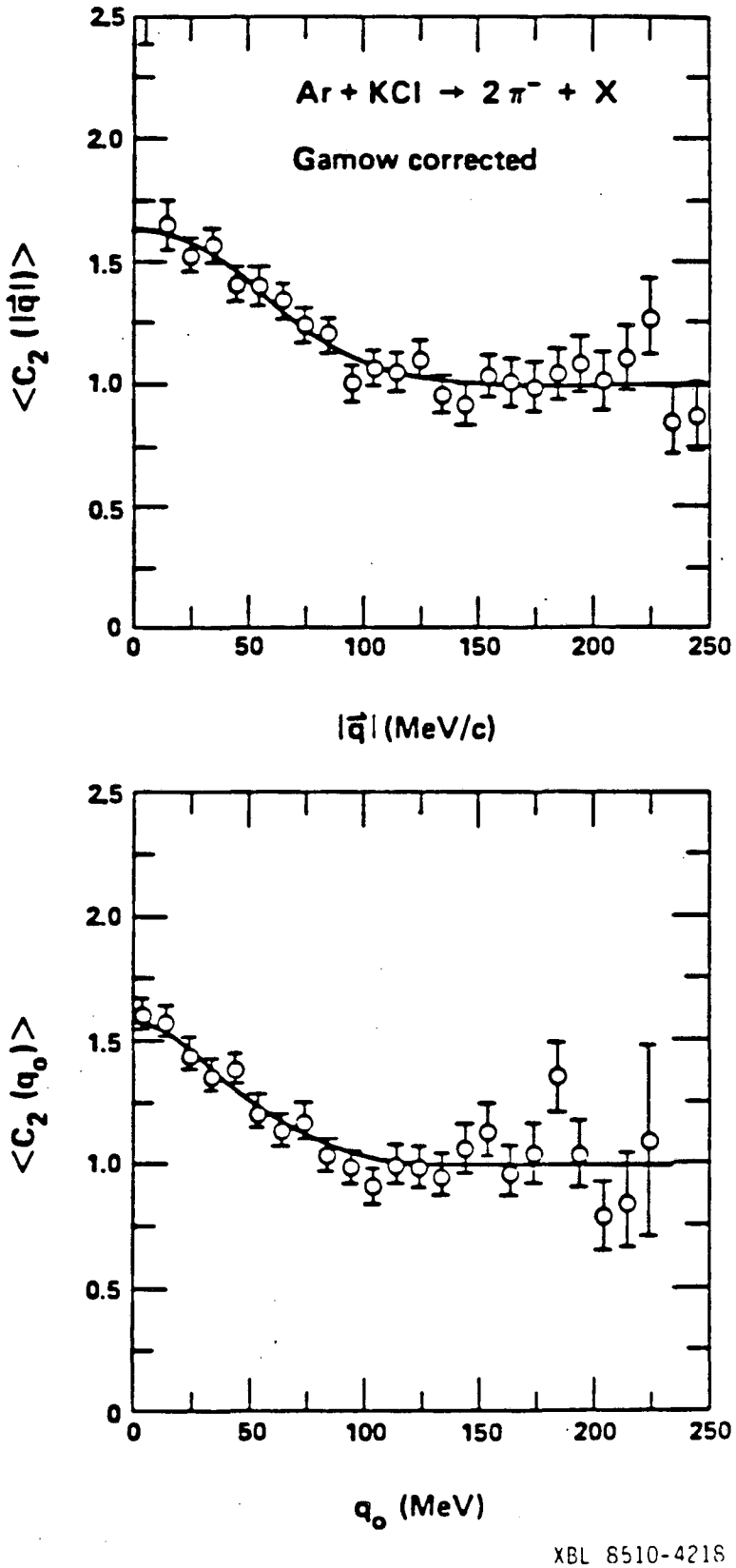
Ar + KCl → 2 π⁻ + X
Gamow corrected
<C2 (|q⃗|)>
|q⃗| (MeV/c)
<C2 (q0)>
q0 (MeV)
0
0.5
1.0
1.5
2.0
2.5
50
100
150
200
250
XBL 8510-4218

Figure 9

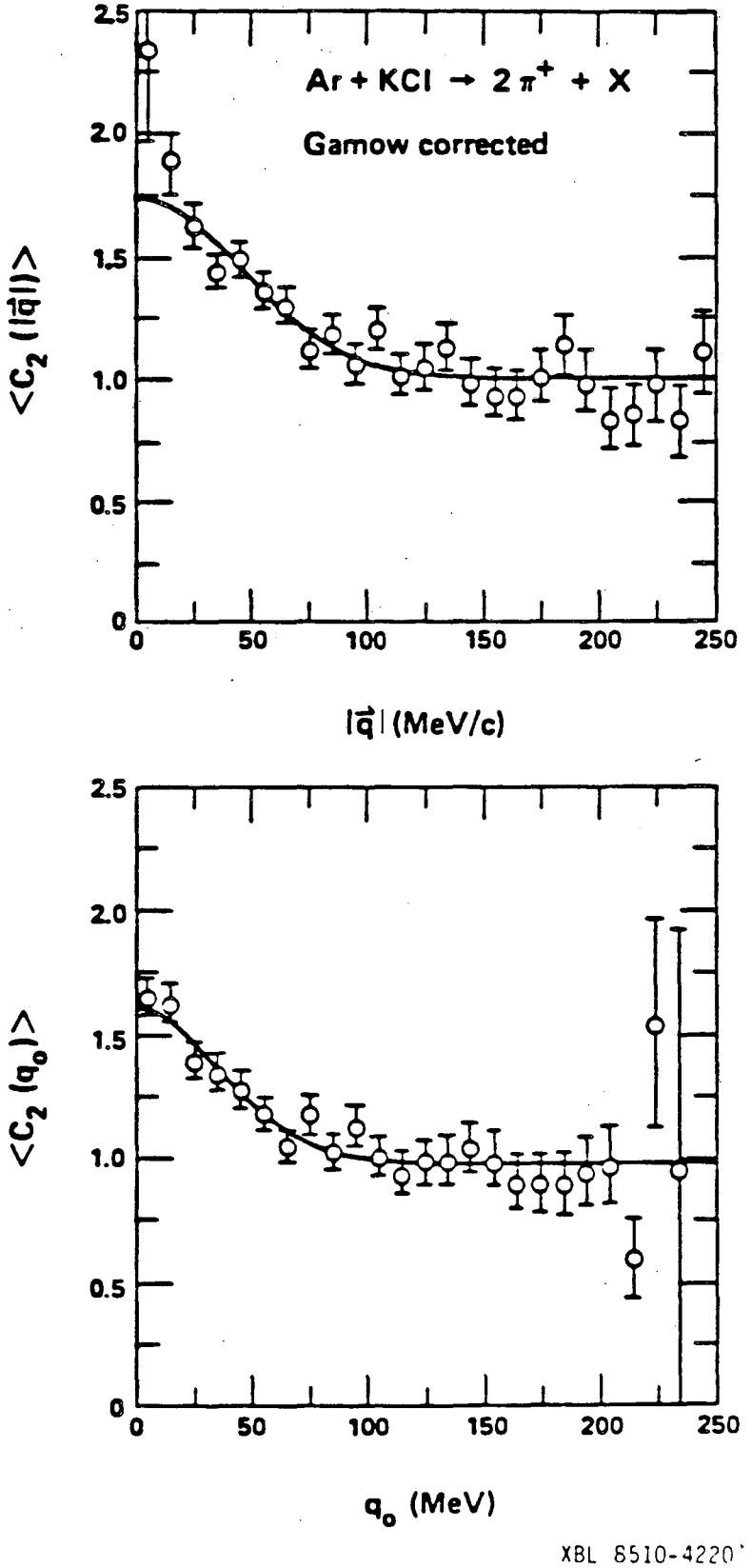
Ar + KCl → 2 π+ + X
Gamow corrected
<C2 (|q⃗|)>
|q⃗| (MeV/c)
<C2 (q0)>
q0 (MeV)
0
0.5
1.0
1.5
2.0
2.5
50
100
150
200
250
XBL 8510-4220

Figure 10

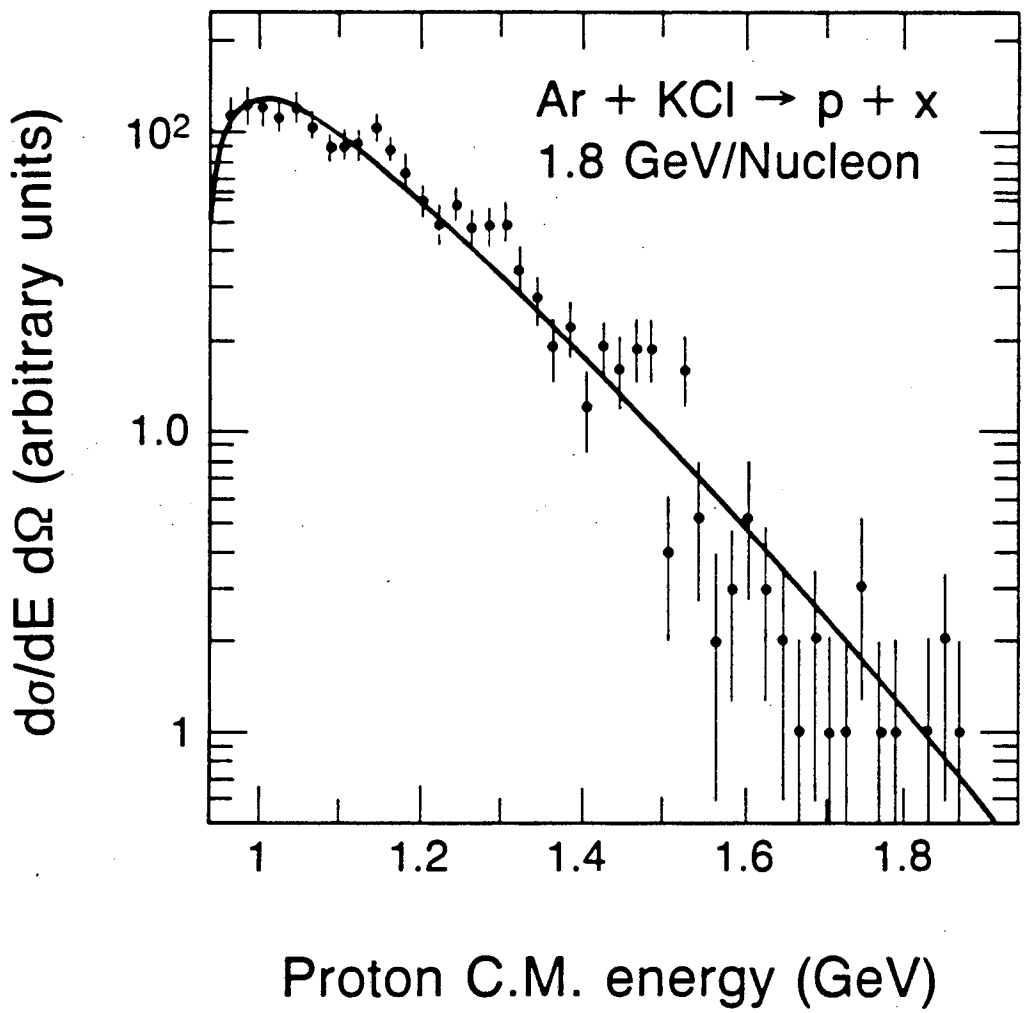

XBL 844-10398

Figure 11

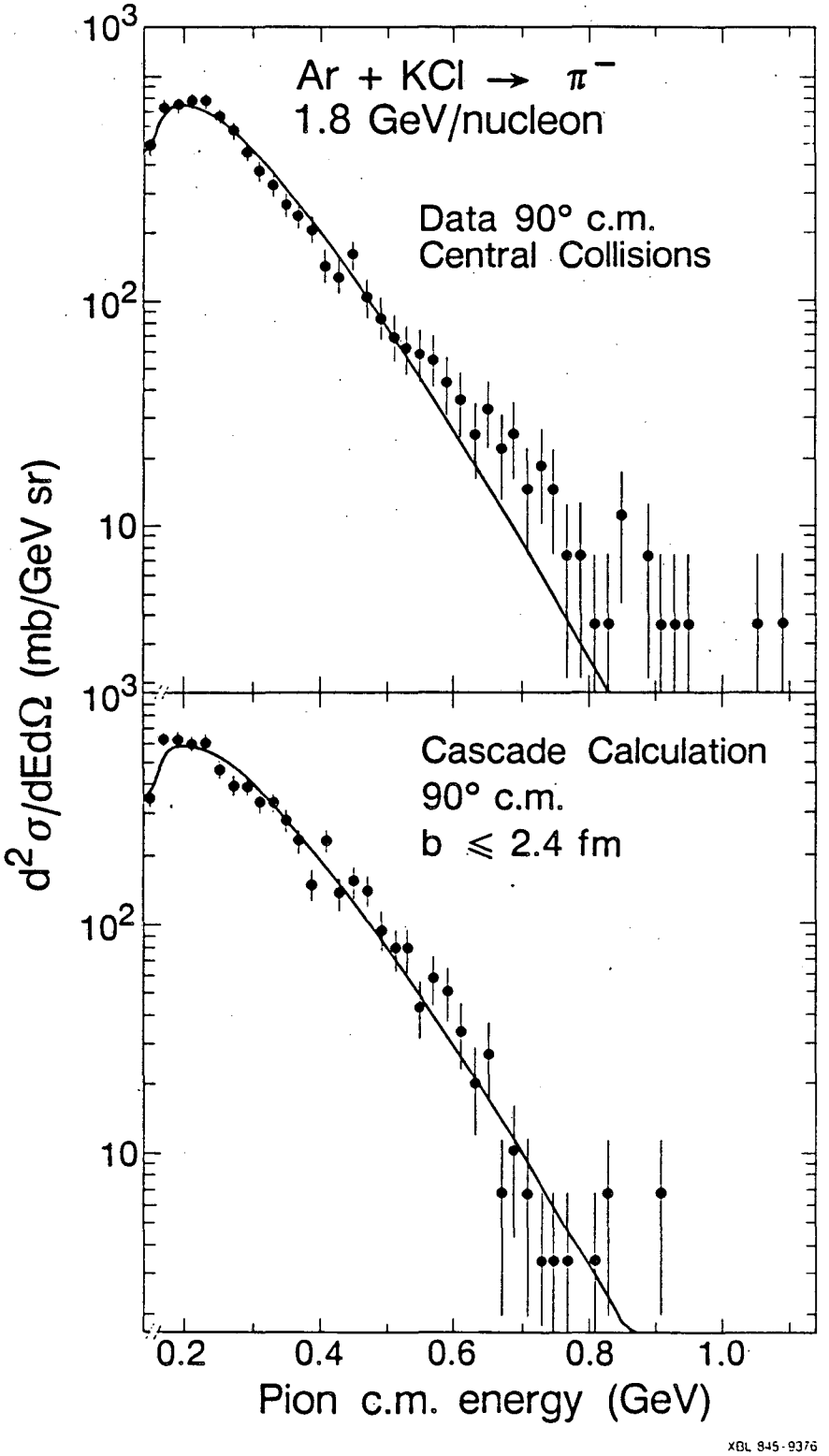
Ar + KCl → π⁻
1.8 GeV/nucleon
Data 90° c.m.
Central Collisions
Cascade Calculation
90° c.m.
b ≤ 2.4 fm
d²σ/dEdΩ (mb/GeV sr)
Pion c.m. energy (GeV)
XBL 845-9376

Figure 12

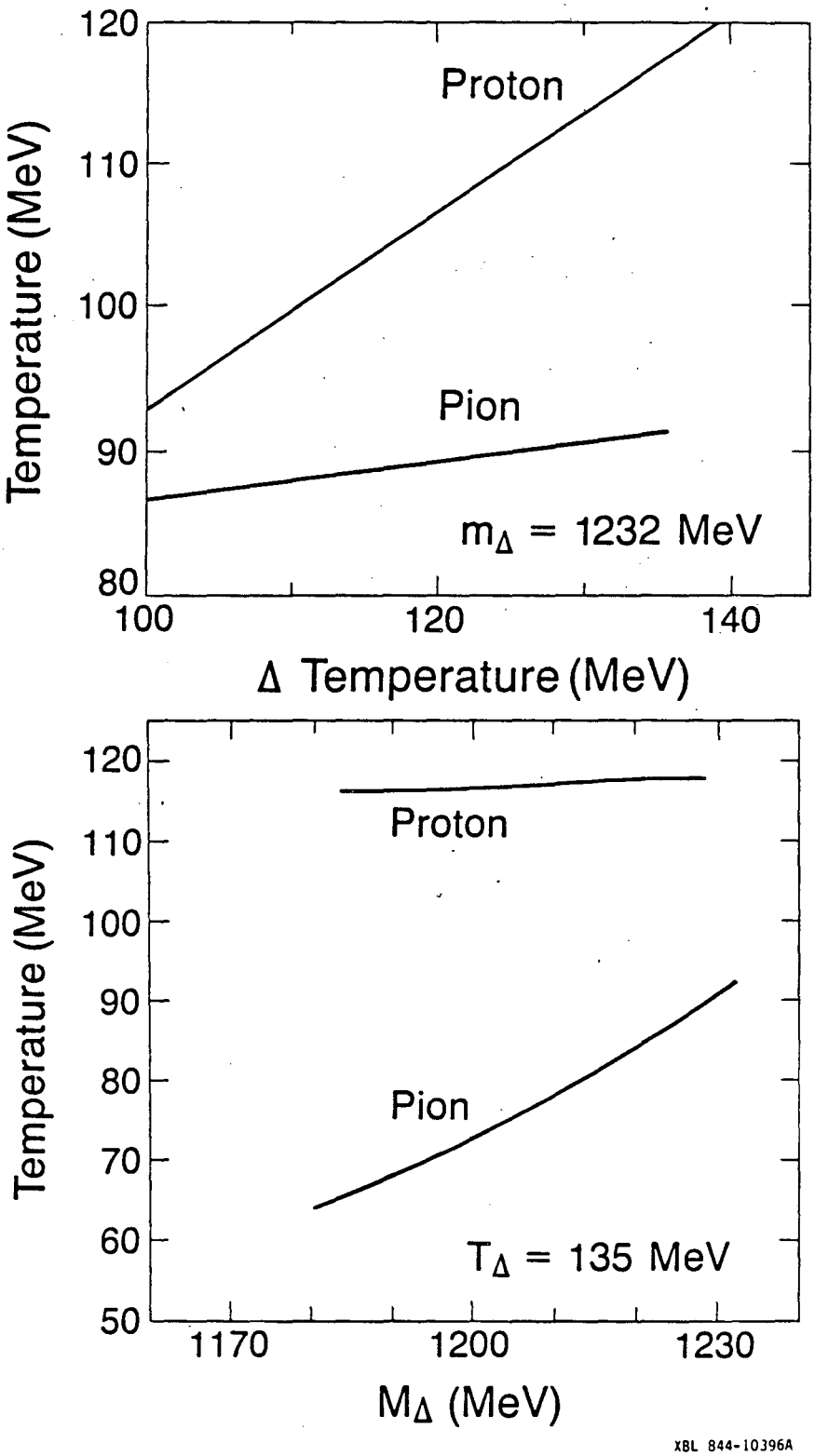
120
110
100
90
80
Temperature (MeV)
Proton
Pion
m_Δ = 1232 MeV
100
120
140
Δ Temperature (MeV)
120
110
100
90
80
70
60
50
Temperature (MeV)
Proton
Pion
T_Δ = 135 MeV
1170
1200
1230
M_Δ (MeV)
XBL 844-10396A

Figure 13

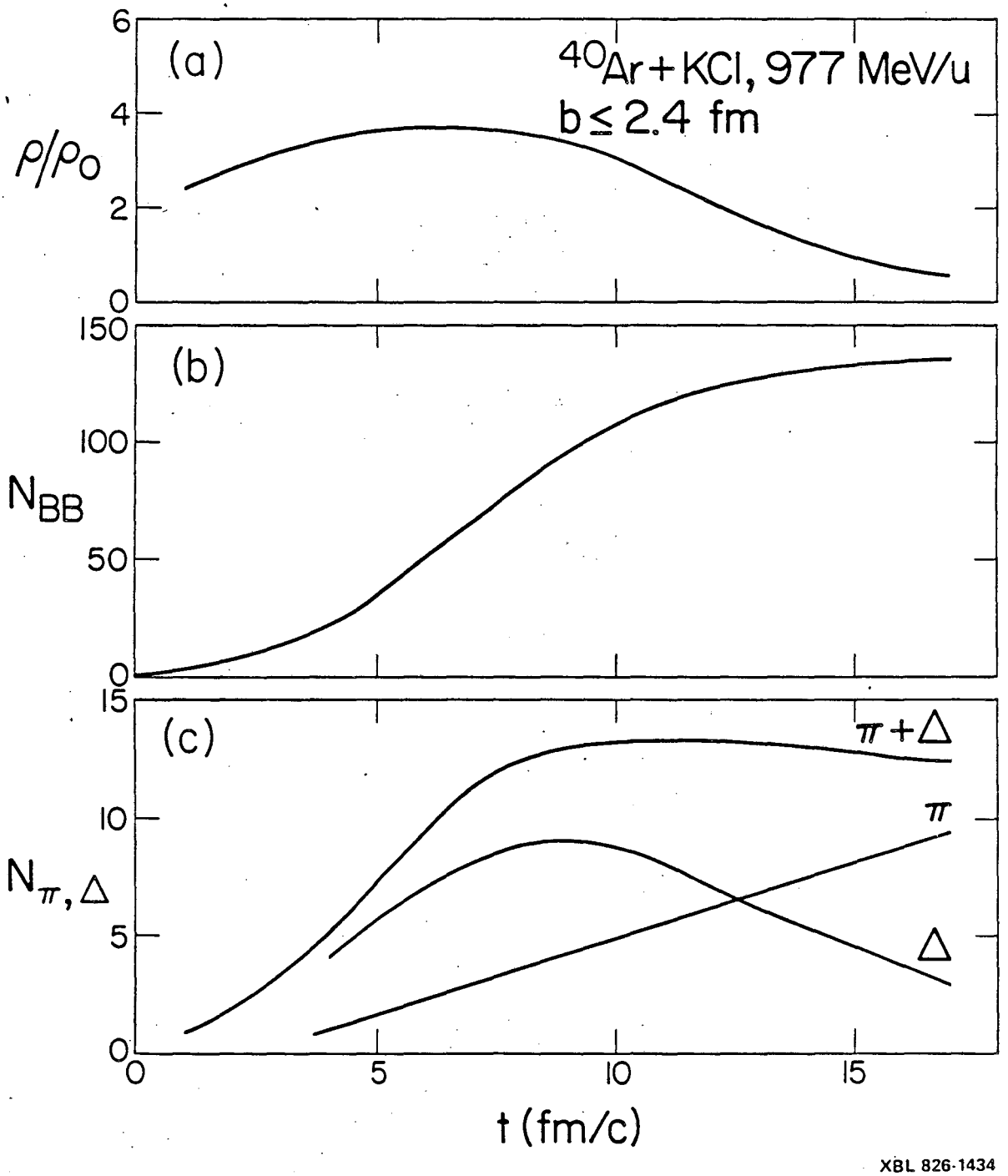

XBL 826-1434

Figure 14

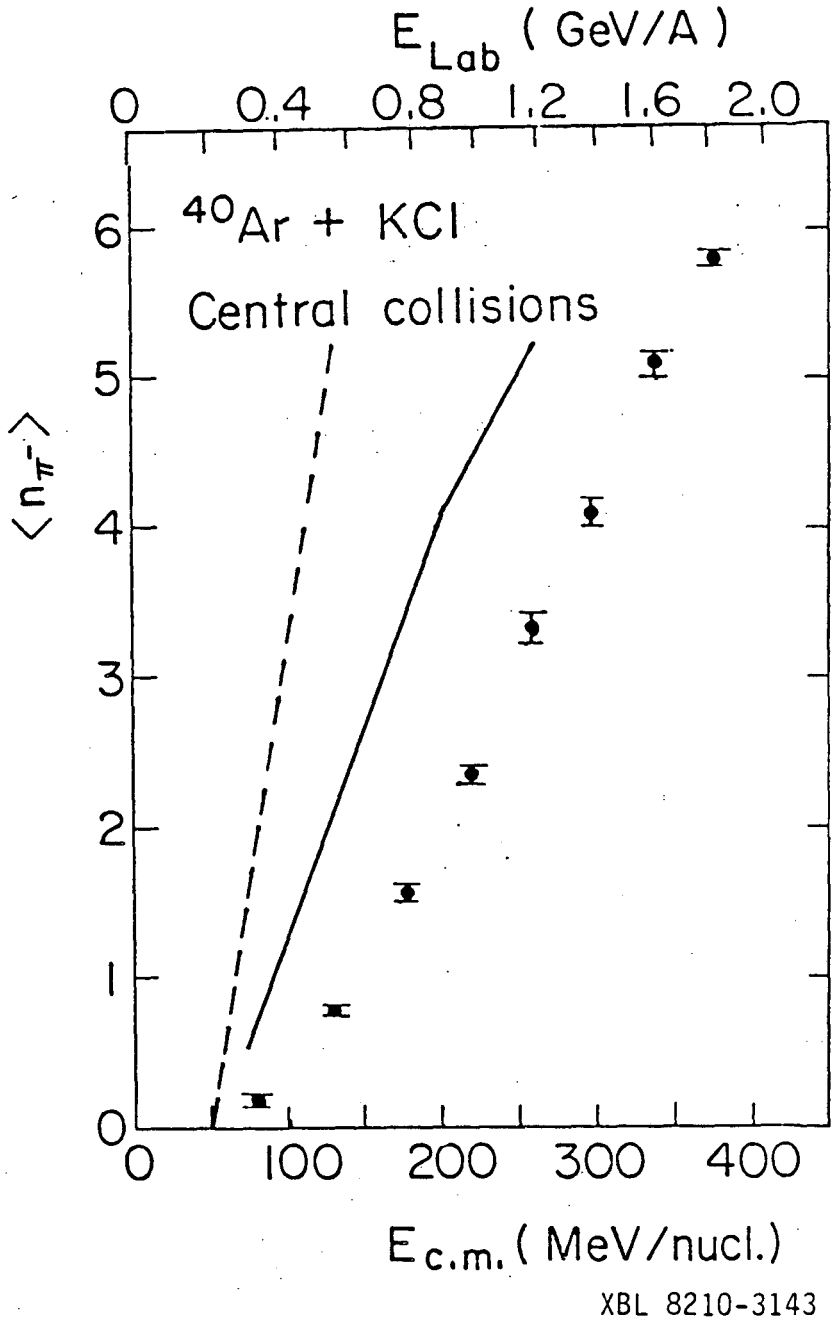
E Lab (GeV/A)
0
0.4
0.8
1.2
1.6
2.0
40Ar + KCl
Central collisions
<nπ->
0
1
2
3
4
5
6
0
100
200
300
400
E c.m. (MeV/nucl.)
XBL 8210-3143

Figure 15

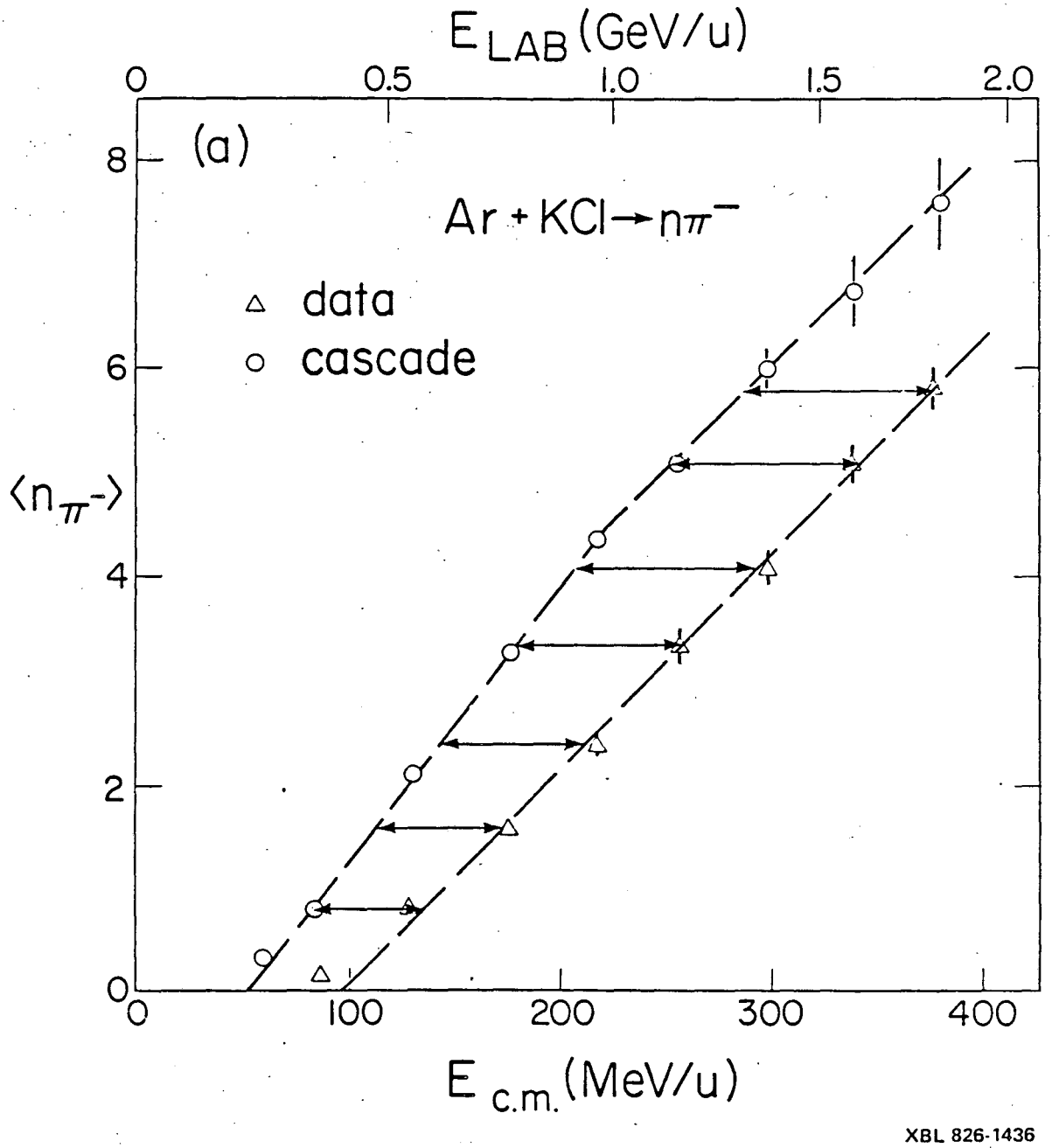
E LAB (GeV/u)
0
0.5
1.0
1.5
2.0
(a)
Ar + KCl → nπ⁻
data
cascade
⟨nπ⁻⟩
0
2
4
6
8
0
100
200
300
400
E c.m. (MeV/u)
XBL 826-1436

Figure 16

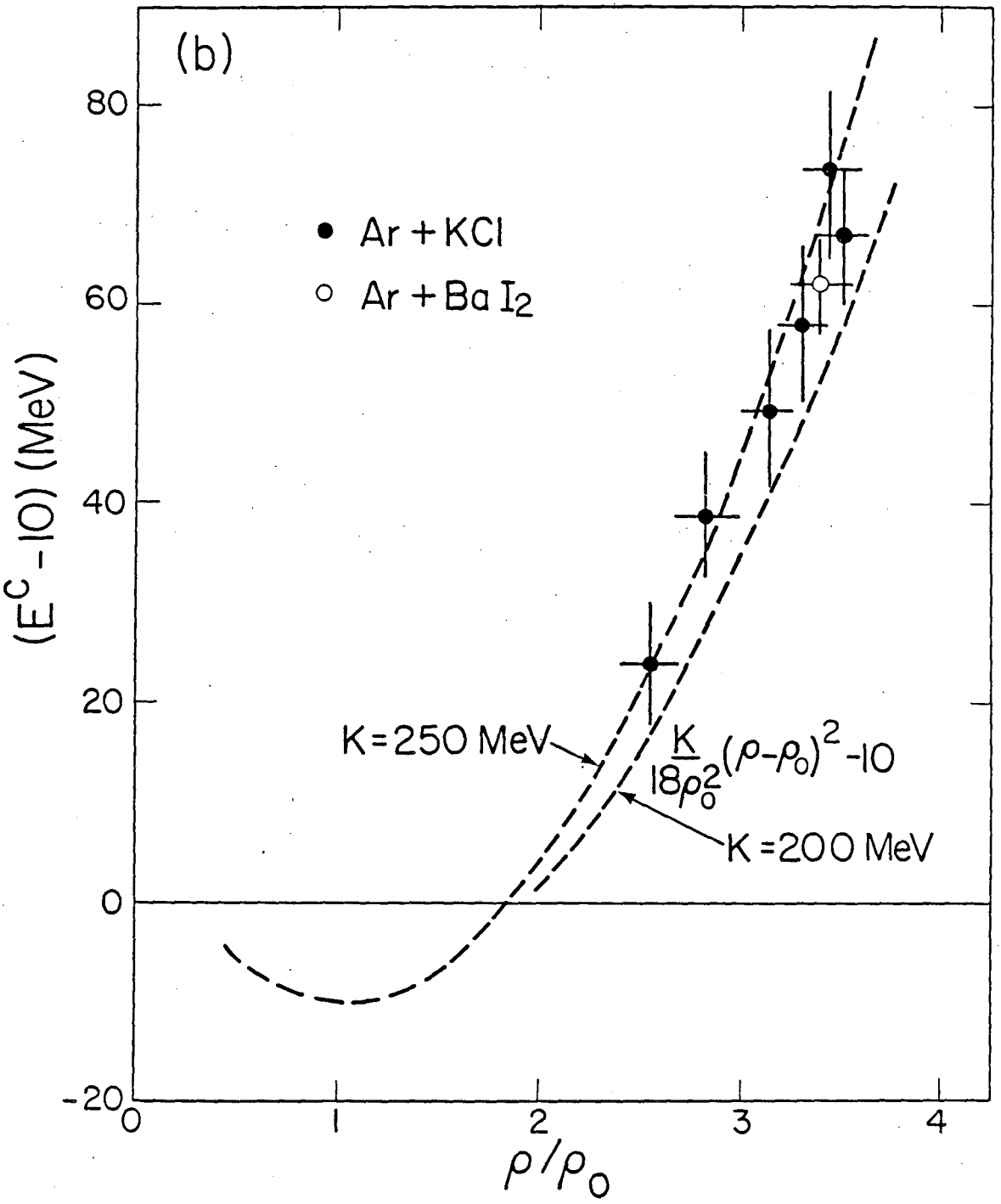
(b)
80
60
40
20
0
-20
0
1
2
3
4
$(E^c - 10)$ (MeV)
ρ/ρ_0
● Ar + KCl
○ Ar + Ba I_2
K = 250 MeV
$\frac{K}{18\rho_0^2}(\rho-\rho_0)^2 - 10$
K = 200 MeV
XBL 826-1435

Figure 17

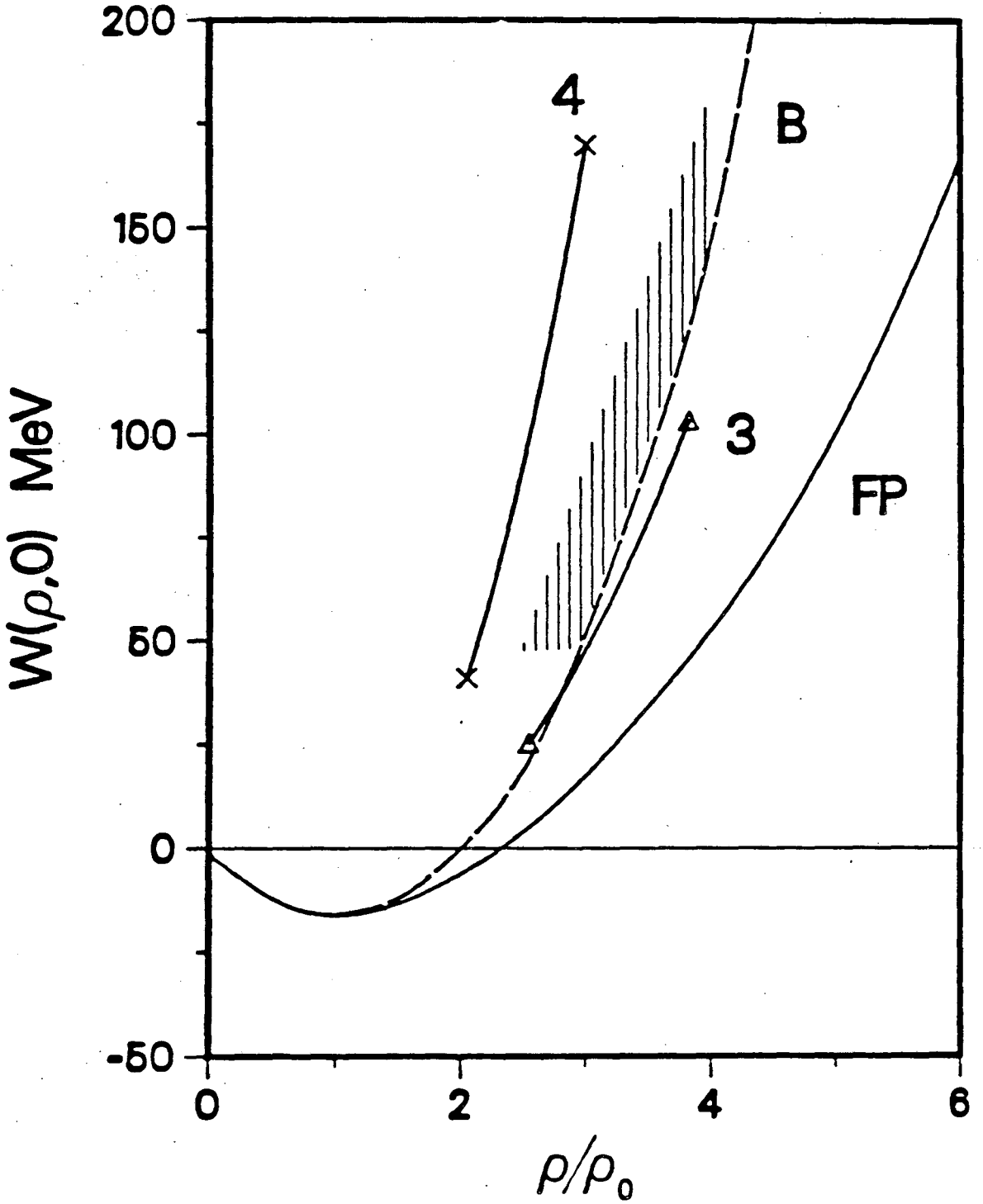

XBL 8510-4219

Figure 18

This report was done with support from the Department of Energy. Any conclusions or opinions expressed in this report represent solely those of the author(s) and not necessarily those of The Regents of the University of California, the Lawrence Berkeley Laboratory or the Department of Energy.

Reference to a company or product name does not imply approval or recommendation of the product by the University of California or the U.S. Department of Energy to the exclusion of others that may be suitable.

LAWRENCE BERKELEY LABORATORY
TECHNICAL INFORMATION DEPARTMENT
UNIVERSITY OF CALIFORNIA
BERKELEY, CALIFORNIA 94720